Macromolecular Rapid Communications
www.mrc-journal.de

The Role of Polymer–AuNP Interaction in the Stimuli-Response Properties of PPA–AuNP Nanocomposites

*Manuel Núñez-Martínez, Sandra Arias, Julián Bergueiro, Emilio Quiñoá, Ricardo Riguera, and Félix Freire**

The helical sense control of dynamic helical polymers such as poly(phenylacetylene)s (PPAs) is greatly affected when they are conjugated to AuNPs through a strong thiol-Au connection, which restricts conformational changes at the polymer. Thus, the classical thiol-MNP bonds must be replaced by weaker ones, such as supramolecular amide–Au interactions. A straightforward preparation of the PPA–Au nanocomposite by reduction of a preformed PPA–Au^{3+} complex cannot be used due to a redox reaction between the two components of the complex which degrades the polymer. To avoid the interaction between the PPA and the Au^{3+} ions before the reduction takes place, the metal ions are added to the polymer solution capped as a TOAB complex, which keeps the PPA stable due to the lack of PPA–Au^{3+} interactions. Ulterior reduction of the Au^{3+} ions by $NaBH_4$ affords the desired nanocomposite, where the AuNPs are stabilized by supramolecular anilide–AuNPs interactions. By using this approach, 3.7 nm gold nanoparticles are generated and aligned along the polymer chain with a regular distance between particles of 6 nm that corresponds to two helical pitches. These nanocomposites show stimuli-responsive properties and are also able to form macroscopically chiral nanospheres with tunable size.

1. Introduction

Metal nanoparticles (MNPs) have been deeply studied during the last decades due to their applications in fields such as sensing,[1] biomedicine,[2,3] and catalysis,[4] among others. MNPs can be prepared using different protocols that usually affect their size and shape.[5,6] Moreover, depending on the structural characteristics of the organic molecules used as protecting agents or coatings—small molecules/polymers, charged/neutral, hydrophobic/hydrophilic, etc.—other properties in addition to the size or shape of the particles may also be affected, such as stability, solubility, or biocompatibility. In the literature, there are several examples of nanocomposites that combine helical macromolecules with relevant biological functions (proteins or DNA) with MNPs.[7–9] In those cases, the helical sense of the biomacromolecule in the composite is fixed and determined by the chirality of the residues used to build the macromolecule. However, the preparation of more appealing nanocomposites made of dynamic helical polymers[10–38]—such as poly(phenylacetylene)s (PPAs)—and MNPs, has been scarcely explored.[39–41] These polymers can tune their helical structure—sense and/or elongation—using different external stimuli such as metal ions, solvent polarity, or temperature, and therefore can provide interesting properties to the nanocomposites. However, depending on the protocol used to prepare the nanocomposite, the dynamic behavior of the polymer can be largely affected. Thus, the dynamic behaviors of PPAs such as poly-(*R*)-**1** that bears the 4-anilide of (*R*)-*α*-methoxy-*α*-phenylacetic acid as pendant group, or poly-(*R*)-**2**, that bears the 4-benzamide of (*S*)-phenylglycine methyl ester as pendant are dramatically reduced when the polymers are attached to a metal nanoparticles through the use of thiol-metal bonds—i.e., poly-[(*R*)-**1**-*co*-thiol-MNP] nanocomposite (M = Au or Ag)—to form the nanocomposites.[39] This problem was surpassed by using supramolecular chemistry to link the PPA to the metal nanoparticle instead of a more "covalent bonds" such as a thiol-Au/Ag linkage. Thus, weak amide–AgNPs interactions between the PPA and the metal nanoparticle, which is found in other polymer-based nanocomposites such as polyvinylpyrrolidone (PVP)-MNPs nanocomposites were employed. To prepare this poly-(*R*)-**1**-AgNPs/dodecanethiol nanocomposites, poly-(*R*)-**1** was complexed with Ag^+ by adding $AgClO_4$ as a source of silver ions, and this complex was further transformed into the poly-(*R*)-**1**-AgNPs/dodecanethiol nanocomposites using $NaBH_4$ as reducing agent and 1-dodecanethiol as costabilizing agent. The resulting nanocomposites show low-polydisperse 2.8 nm AgNPs linearly distributed along the PPA chain. This weak supramolecular interaction between PPA and AgNP allows preserving the dynamic behavior of poly-(*R*)-**1** within the nanocomposite, where *P* or *M* helical senses can be effectively induced in the helical

M. Núñez-Martínez, S. Arias, J. Bergueiro, E. Quiñoá, R. Riguera, F. Freire
Centro Singular de Investigación en Química Biolóxica e Materiais Moleculares (CiQUS) and Departamento de Química Orgánica
Universidade de Santiago de Compostela
E-15782 Santiago de Compostela, Spain
E-mail: felix.freire@usc.es

DOI: 10.1002/marc.202100616

polymer by action of external stimuli.[40] Thus, while strong polymer-metal nanoparticle interactions inhibit the dynamic behavior of the nanocomposite,[39] weak supramolecular forces preserve it.[40] Herein, we will explore the formation of poly-(*R*)-**1**-AuNPs/dodecanethiol nanocomposites, where supramolecular amide–AuNP interactions are used to link both components of the nanocomposite.

2. Results and Discussion

In a first attempt, the preparation of poly-(*R*)-**1**-AuNPs/dodecanethiol nanocomposite was carried out using the protocol developed for poly-(*R*)-**1**-AgNPs/dodecanethiol nanocomposite.[40] Thus, 0.5 equiv of a methanolic solution of $HAuCl_4$ were added to a chloroform solution of poly-(*R*)-**1** (0.3 mg mL^{-1}) to form a poly-(*R*)-**1**/Au^{3+} complex (**Figure 1**a). A color change from yellow to blue is observed once the metal ion is added to the polymer solution (Figure 1b).

EPR studies revealed the presence of a radical specie in the polymer, which is delocalized along the polyene backbone (Figure 1d) and generated by a redox process after the addition of the Au^{3+} ions. The generation of radical species must be avoided in PPAs due to a *cis* to *trans* isomerization of the polyene backbone, that results in a planarization of the polymer, and where nonhelical structures can be generated. XPS experiments demonstrated a redox process when poly-(*R*)-1 and Au^{3+} ions are mixed. Thus, Au^{3+} is partially reduced to Au^0 signals generating a radical cation in the PPA as inferred previously by EPR studies (Figure 1e). On the other hand, transmission electron microscopy (TEM) images of the PPA/Au^{3+} mixture show the presence of polydisperse AuNPs and with different morphology, conforming this redox process (Figure 1c; Figure S5, Supporting Information).

Thus, an alternative protocol must be developed to prepare the poly-(*R*)-**1**-AuNPs/dodecanethiol nanocomposite, avoiding a direct complexation between the polymer and the Au^{3+} ions. To surpass this problem, we decided to inhibit the redox reaction by deactivation of the Au^{3+} ions. To do that, a variation of the Brust-Schiffrin[42] protocol was used to prepare the poly-(*R*)-**1**-AuNPs/dodecanethiol nanocomposite. First, tetraoctylammonium bromide was used to transfer the Au^{3+} ions from an aq $HAuCl_4$ solution to an organic solvent, in this case dichloromethane. Next, poly-(*R*)-**1** and 1-dodecanethiol were added at a Au^{3+}/ poly-(*R*)-**1**/1-dodecanethiol ratio of 1/0.4/0.8 (mol/mol/mol) to the organic layer and the mixture was stirred for 20 min at −4 °C before adding the reducing agent.

In this solution mixture, 1-dodecanethiol interacts with the Au^{3+} to form a stable complex, which avoids the PPA–Au^{3+} interaction and the polymer denaturalization. Next, $NaBH_4$ was added to the dichloromethane solution and the reaction mixture turned from yellow/orange towards brown/black color, indicating the generation of AuNPs (**Figure 2**a).

The resulting material was purified by precipitation with toluene and centrifugation (see more details in the Supporting Information). Further purification of the nanocomposite was carried out by gel performance chromatography (GPC), which showed the presence of a GPC peak (t_R poly-(*R*)-**1**-AuNPs/dodecanethiol = 10 min, Figure 2d) with shorter t_R than those obtained for the starting components—t_R poly-(*R*)-**1** = 21 min; t_R AuNPs = 27 min—(see ESI Figure S13 in the Supporting Information). Moreover, additional GPC studies at two different wavelengths—540 (LSPR absorption) and 380 nm (polymer absorption)—showed the formation of the nanocomposite, which absorbs at those wavelengths, while the parent components, poly-(*R*)-**1** and AuNPs absorb at 380 and 540 nm respectively (Figure S13, Supporting Information).

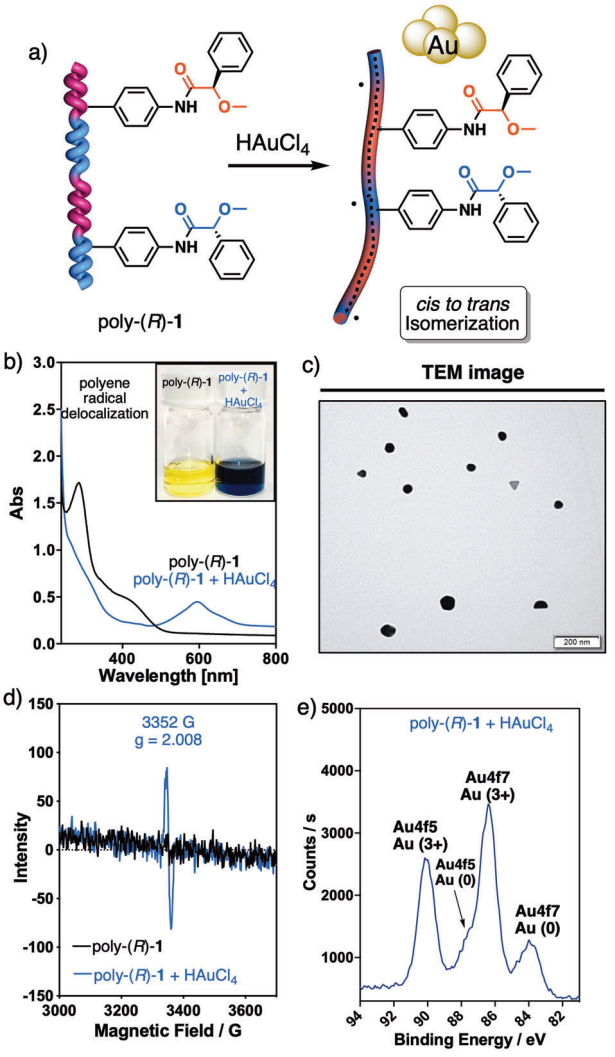

Figure 1. a) Schematic representation for the formation of radicals in poly-(*R*)-**1** in presence of $HAuCl_4$. b) UV–vis spectra of poly-(*R*)-**1** and poly-(*R*)-**1** in presence of $HAuCl_4$. c) TEM images of AuNPs generated by the redox process. d) EPR studies of poly-(*R*)-**1** and poly-(*R*)-**1** in presence of $HAuCl_4$. e) XPS studies of poly-(*R*)-**1** in presence of $HAuCl_4$.

Therefore, these results indicate that while poly-(*R*)-**1** does not interact with Au^{3+}/1-dodecanethiol complexes, the reduction of Au^{3+} to Au^0 promotes the interaction between the three components generating the desired desired poly-(*R*)-**1**-AuNPs/dodecanethiol nanocomposite. This hybrid material exhibits excellent stability and can be stored in solid state under an argon atmosphere for months.

Characterization of the poly-(*R*)-**1**-AuNPs/dodecanethiol hybrid material was done using different techniques such as differential scanning calorimetry (DSC), ^{1}H-NMR, UV–vis, and IR.

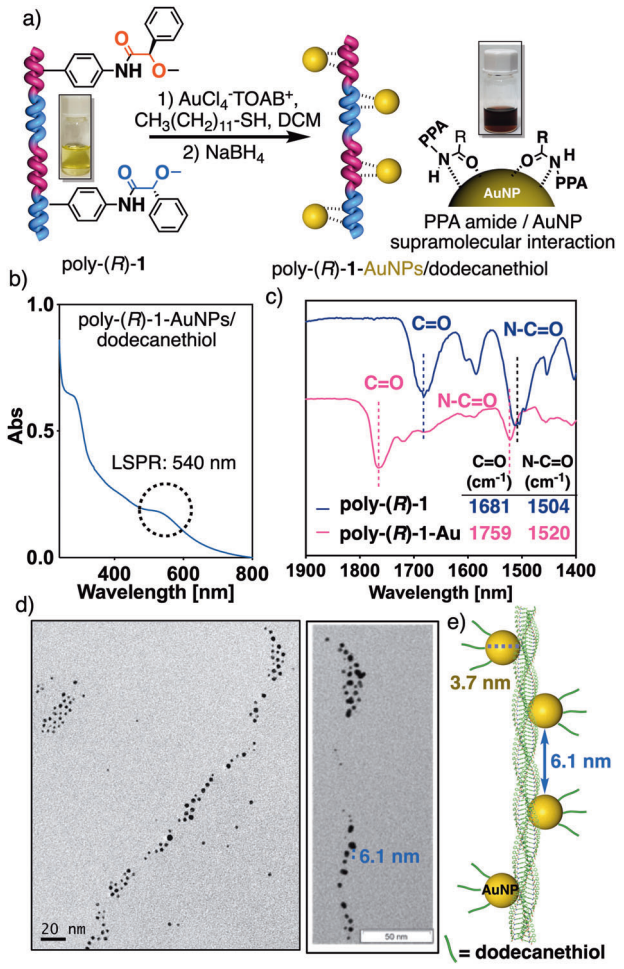

Figure 2. a) Schematic representation for the formation of poly-(*R*)-**1**-AuNPs nanocomposites by a variation of Brust-Schiffrin method. b) UV–vis, c) FT-IR experiments of poly-(*R*)-**1** and poly-(*R*)-**1**-AuNPs/dodecanethiol nanocomposites. d) TEM images of poly-(*R*)-**1**-AuNPs/dodecanethiol nanocomposites (3.7 ± 1.2, 93 nanoparticles). e) Illustration of a poly-(*R*)-**1**-AuNPs/dodecanethiol nanocomposites, showing a linear and random distribution of AuNPS along the polymer chain.

UV–vis measurements showed the characteristic trace of poly-(*R*)-**1** and the presence of an extra UV band at 540 nm corresponding to the localized surface plasmon resonance (LSPR) band of spherical AuNPs (Figure 2b). This fact indicates the presence of the two components in the nanocomposite. ^{1}H-NMR experiments showed the signals corresponding to poly-(*R*)-**1** and 1-dodecanethiol, corroborating therefore the obtention of the nanocomposite (Figure S16, Supporting Information). Interestingly, FT-IR studies showed a strong interaction between the anilide group of poly-(*R*)-**1** and the AuNPs—$\Delta\tilde{\nu}_{CO}$ = 78 cm^{-1}; $\Delta\tilde{\nu}_{NCO}$ = 16 cm^{-1}—fact that indicates as expected the role of the anilide at poly-(*R*)-**1** in the stabilization of the AuNPs (Figure 2c).

Once, the presence of the nanocomposite was demonstrated, structural studies on the polymer were carried out to demonstrate that its helical structure remained unaltered during the formation of the hybrid material. Thus, DSC experiments showed a thermogram characteristic for a *cis-cisoidal* structure, like the one obtained for the parent PPA poly-(*R*)-**1** (Figure S14 in the Supporting Information for details).

To study the morphology of the aggregate, dynamic light scattering (DLS) and electron microscopy studies were carried out. DLS experiments indicated the formation of large aggregates compared to the parent polymer—poly-(*R*)-**1**–(Figure S12 in the Supporting Information). On the other hand, TEM studies produced images that showed the presence of small, spherical, low-polydisperse AuNPs (3.7 ± 1.2 nm), which are aligned along the polymer chain and regularly separated ≈6.1 nm that coincide with two consecutive helical pitches of poly-(*R*)-**1** (Figure 2d and Supporting Information).

Next, the dynamic behavior of the helical polymer within the nanocomposites was analyzed by electron circular dichroism (ECD) and stimuli responsive studies. These experiments allow determining how the different helical enhancement effects observed in poly-(*R*)-**1** are affected once poly-(*R*)-**1**-AuNPs/dodecanethiol is prepared. To do that, ECD experiments of a poly-(*R*)-**1**-AuNPs/dodecanethiol nanocomposite dispersion prepared in chloroform (0.1 mg mL^{-1}) were carried out. As expected, the ECD trace was null in the 300–500 nm region, which indicates the presence of an axially racemic polymer within the nanocomposite (see ESI).

The addition of external stimuli such as monovalent (Li^+) or divalent (Ba^{2+}) metal ions in a poly-(*R*)-**1**-AuNPs/dodecanethiol/M^{n+} 1.0/0.5 mol/mol ratio induce either *M* ($CD_{380} < 0$) or *P* ($CD_{380} > 0$) helix in the PPA similar to those reported previously for poly-(*R*)-**1** (**Figure 3**b; Figure S19, Supporting Information). Comparison of the ECD traces obtained for poly-(*R*)-**1**-AuNPs/dodecanethiol/Ba^{2+} and poly-(*R*)-**1**-AuNPs/dodecanethiol/Li^+ with those obtained for poly-(*R*)-**1**/Ba^{2+} and poly-(*R*)-**1**/Li^+ shows that the helical sense induction in the nanocomposite/metal complex is smaller than in the polymer/metal complex (Figure 3b,c). In this case, a depletion of ca. 40% of the helix enhancement effect for poly-(*R*)-**1** in the nanocomposite is observed, which is associated to a strong supramolecular interaction between the anilide groups and the gold nanoparticles.

Finally, the formation of nanospheres based on poly-**1**-AuNPs/dodecanethiol/M^{n+} was explored using metal ions that act as crosslinking agents. Thus, dispersions of poly-(*R*)-**1**-AuNPs/dodecanethiol/Ba^{2+} complexes (0.1 mg mL^{-1}) at different mol/mol ratios (1/0.2, 1/0.4, and 1/0.6) were prepared and studied by DLS and surface electron microscopy (SEM). These studies manifest the presence of nanospheres, whose size and macroscopic chiral content (excess of *M* or *P* helical sense) can be tuned by varying the amount of metal in the complex (Figure 3d,e; Figure S20 for more details in the Supporting Information).

3. Conclusion

In conclusion, it was demonstrated that it is possible to prepare dynamic chiral nanocomposites based on supramolecular interactions between PPAs and gold nanoparticles—AuNP–anilide interactions. To prepare these nanocomposites, a variation of the Brust–Schiffrin protocol is necessary to avoid the degradation of the PPA by Au^{3+} ions. In this case, TOAB is first complexed to

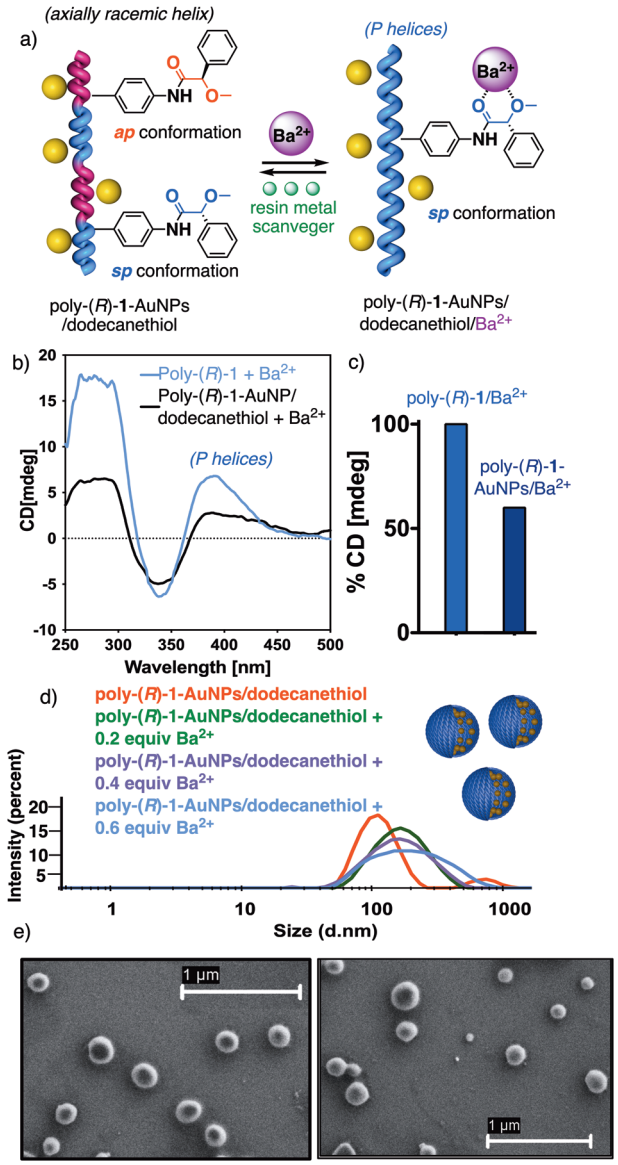

Figure 3. a) Schematic representation of helical induction by adding Ba^{2+} to poly-(*R*)-**1**-AuNPs/dodecanethiol nanocomposites. b) CD traces for poly-(*R*)-**1**/Ba^{2+} and poly-(*R*)-**1**-AuNPs/dodecanethiol/Ba^{2+} at 0.1 mg mL^{-1} in $CHCl_3$. c) Representation of % CD intensity at 380 nm for poly-(*R*)-**1**/Ba^{2+} and poly-(*R*)-**1**-AuNPs/dodecanethiol/Ba^{2+}. d) DLS measurements for poly-(*R*)-**1**-AuNPs/dodecanethiol/Ba^{2+} at 0.1 mg mL^{-1} in $CHCl_3$. e) SEM images for poly-(*R*)-**1**-AuNPs/dodecanethiol/Ba^{2+} in a mol/mol ratio (1/0.4) (Size: 200 ± 24 nm, 23 particles).

Au^{3+} ions, then poly-(*R*)-**1** and the reducing agents are added producing the nanocomposites which contain small and low polydisperse AuNPs (3.7 ± 1.2 nm). These AuNPs line up along the polymer chain and are regularly displayed at ≈6 nm, a distance that corresponds to two consecutive helical pitches.

These studies confirm that to prepare a dynamic helical polymer-MNP nanocomposite it is necessary to consider how the strength of the PPA–MNP interaction affects its dynamic behavior. Thus, while strong thiol–AuNP interactions reduce dramatically the dynamic behavior of the PPA, weaker supramolecular interactions maintain good stimuli response properties in the nanocomposite.

These studies are a breakthrough in the development of novel hybrid materials based on dynamic helical polymers, providing rules on how to attach these polymers to other materials, not just metal nanoparticles, without affecting their dynamic behavior. Finally, the preparation of these chiral nanocomposites open new possibilities in the preparation of materials with dynamic chiral plasmon response, where the dynamic character of the PPA could be transferred to the metal nanoparticles.

Supporting Information

Supporting Information is available from the Wiley Online Library or from the author.

Acknowledgements

The authors thank Servicio de Microscopía Electrónica (RIAIDT, USC) and Servicio de Nanotecnología y Análisis de Superficies (CACTI, UVIGO). Financial support from AEI (PID2019-109733GB-I00), Xunta de Galicia (ED431C 2018/30, Centro Singular de Investigación de Galicia acreditación 2019–2022, ED431G 2019/03, Beca Leonardo a Investigadores y Creadores Culturales 2020 de la Fundación BBVA and the European Regional Development Fund (ERDF) and is gratefully acknowledged. N.-M. thanks MICINN for a FPI contract (BES-2016-078107).

Conflict of Interest

The authors declare no conflict of interest.

Data Availability Statement

Data available in article supplementary material

Keywords

chirality, gold nanoparticles, helical polymers, nanocomposites

Received: September 22, 2021
Revised: October 26, 2021
Published online: November 17, 2021

[1] S. Zhang, R. Geryak, J. Geldmeier, S. Kim, V. Tsukruk, *Chem. Rev.* **2017**, *117*, 12942.
[2] M. Molina, M. Asadian-Birjand, J. Balach, J. Bergueiro, E. Miceli, M. Calderon, *Chem. Soc. Rev.* **2015**, *17*, 6161.
[3] M. Carril, D. Padro, P. del Pino, C. Carrillo-Carrion, M. Gallego, J. W. Parak, *Nat. Commun.* **2017**, *8*, 1542.
[4] Y. Zhou, H. Sun, S. Matysiak, J. Ren, X. Qu, *Angew. Chem., Int. Ed.* **2018**, *57*, 16791.
[5] G. Zheng, Z. Bao, J. Pérez-Juste, D. Ruolan, W. Liu, J. Dai, W. Zhang, L. Lee, K. Y. Wong, *Angew. Chem., Int. Ed.* **2018**, *57*, 16452.
[6] A. Sánchez-Iglesias, X. Zhuo, W. Albrecht, S. Bals, L. Liz-Marzán, *ACS Mater. Lett.* **2020**, *2*, 1246.

[7] J. Mosquera, Y. Zhao, H. J. Jang, N. Xie, C. Xu, N. Kotov, L. M. Liz-Marzán, *Adv. Funct. Mater.* **2020**, *30*, 1902082.
[8] C. Pigliacelli, R. Sánchez-Fernández, M. D. García, C. Peinador, E. Pazos, *Chem. Commun.* **2020**, *56*, 8000.
[9] J. Lu, Y. Xue, K. Bernardino, N. N. Zhang, W. R. Gomes, N. S. Ramesar, S. Liu, Z. Hu, T. Sun, A. Farias de Moura, N. A. Kotov, K. Liu, *Science* **2021**, *371*, 1368.
[10] E. Yashima, K. Maeda, H. Lida, Y. Furusho, K. Nagai, *Chem. Rev.* **2009**, *109*, 6102.
[11] E. Yashima, K. Maeda, *Macromolecules* **2008**, *41*, 3.
[12] B. M. Rosen, C. J. Wilson, D. A. Wilson, M. Peterca, M. R. Imam, V. Percec, *Chem. Rev.* **2009**, *109*, 6275.
[13] F. Freire, E. Quiñoá, R. Riguera, *Chem. Rev.* **2016**, *116*, 1242.
[14] F. Freire, J. M. Seco, E. Quiñoá, R. Riguera, *J. Am. Chem. Soc.* **2012**, *134*, 19374.
[15] X. Guan, S. Wang, G. Shi, J. Zhang, X. Wan, *Macromolecules* **2021**, *54*, 4592.
[16] H. Huang, H. Duan, L. Yin, D. Qi, J. Xue, Y. Zhang, J. Deng, *Macromolecules* **2020**, *53*, 6002.
[17] E. Suárez-Picado, E. Quiñoá, R. Riguera, F. Freire, *Chem. Mater.* **2018**, *30*, 6908.
[18] S. Arias, M. Núñez-Martinez, E. Quiñoá, R. Riguera, F. Freire, *Polym. Chem.* **2017**, *8*, 3740.
[19] K. Echizen, T. Taniguchi, T. Tatsuya Nishimura, K. Maeda, *J. Am. Chem. Soc.* **2021**, *143*, 3604.
[20] M. Alzubi, S. Arias, I. louzao, E. Quiñoá, R. Riguera, F. Freire, *Chem. Commun.* **2017**, *53*, 8573.
[21] F. Rey-Tarrío, R. Rodríguez, E. Quiñoá, R. Riguera, F. Freire, *Angew. Chem., Int. Ed.* **2021**, *60*, 8095.
[22] Z. Fernández, B. Fernández, E. Quiñoá, R. Riguera, F. Freire, *Chem. Sci.* **2020**, *11*, 7182.
[23] S. Arias, M. Nuñez-Martínez, E. Quiñoá, R. Riguera, F. Freire, *Small* **2017**, *13*, 1602398
[24] T. Ikai, T. Kurake, S. Okuda, K. Maeda, E. Yashima, *Angew. Chem., Int. Ed.* **2021**, *60*, 4625.
[25] L. Zhou, L. Chong-Long, G. Run-Tan, K. Shu-Ming, X. Lei, X. Xun-Hui, L. Na, W. Zong-Quan, *Macromolecules* **2021**, *54*, 679.
[26] R. Rodríguez, E. Suárez-Picado, E. Quiñoá, R. Riguera, F. Freire, *Angew. Chem., Int. Ed.* **2020**, *59*, 8616.
[27] E. Yashima, N. Ousaka, D. Taura, K. Shimomura, T. Ikai, K. Maeda, *Chem. Rev.* **2016**, *116*, 13752.
[28] T. Nakano, Y. Okamoto, *Chem. Rev.* **2001**, *101*, 4013.
[29] E. Schwartz, M. Koepf, H. J. Kitto, R. J. M. Nolte, A. E. Rowan, *Polym. Chem.* **2011**, *2*, 33.
[30] K. Maeda, M. Nozaki, K. Hashimoto, K. Shimomura, D. Hirose, T. Nishimura, G. Watanabe, E. Yashima, *J. Am. Chem. Soc.* **2020**, *142*, 7668.
[31] E. Yashima, K. Maeda, Y. Furusho, *Acc. Chem. Res.* **2008**, *41*, 1166.
[32] R. Ishidate, A. J. Markvoort, K. Maeda, E. Yashima, *J. Am. Chem. Soc.* **2019**, *141*, 7605.
[33] R. Rodríguez, S. Arias, E. Quiñoá, R. Riguera, F. Freire, *Nanoscale* **2017**, *9*, 17752.
[34] M. Alzubi, S. Arias, I. Louzao, E. Quiñoá, R. Riguera, F. Freire, *Chem. Commun.* **2017**, *53*, 8573.
[35] S. Arias, J. Bergueiro, F. Freire, E. Quiñoá, R. Riguera, *Small* **2016**, *12*, 238.
[36] L. Palomo, R. Rodríguez, S. Medina, E. Quiñoá, J. Casado, F. Freire, F. J. Ramírez, *Angew. Chem., Int. Ed.* **2020**, *59*, 9080.
[37] E. Suárez-Picado, E. Quiñoá, R. Riguera, F. Freire, *Angew. Chem., Int. Ed.* **2020**, *59*, 4537.
[38] Y. Li, L. Xu, S. Kang, L. Zhou, N. Liu, Z.- Q. Wu, *Angew. Chem., Int. Ed.* **2021**, *60*, 7174.
[39] J. Bergueiro, M. Nuñez-Martínez, S. Arias, E. Quiñoá, R. Riguera, F. Freire, *Nanoscale Horiz.* **2020**, *5*, 495.
[40] M. Nuñez-Martínez, S. Arias, E. Quiñoá, R. Riguera, F. Freire, *Chem. Mater.* **2021**, *33*, 4805.
[41] C. Zhang, C. Song, W. Yang, J. Deng, *Macromol. Rapid Commun.* **2013**, *34*, 1319.
[42] M. Brust, M. Walker, D. Bethell, D. J. Schiffrin, R. J. Whyman, *Chem. Commun.* **1994**, 801.

